On the descent of the Alpine south foehn

Lukas Jansing et al.

The authors make this review process a real pleasure by so carefully responding to the reviews, undertaking additional analyses, and producing additional figures. Thanks!
The research they undertook is a treasure trove and a few more pieces have been lifted from it in the course of the review process. And a few more will be lifted in the course of what I think will be the last round of the revisions.

Major comments:

1. **Influence of up/downstream air mass difference on descent - up/downstream profiles:** I agree that it is difficult to determine a suitable upstream location for studying the influence of potential temperature differences on foehn descent within the complex topography of the Alps. The Sierra Nevada topography studied by Mayr and Armi (2010) is much simpler. The figures R1 and R2 produced for the response confirm this. I disagree with the authors on parts of their interpretation and urge to choose different upstream and downstream locations for the vertical potential temperature profiles.
   a. **Interpretation:** I attach an annotated version of the authors' Fig. R1 (Fig. A1-R1) and added a crucial missing part: the lowest elevation over which foehn can actually flow (estimated to be around 2.2 km). Contrary to what the response states, it becomes clear that the upstream air can only descend a few hundred meters at the first time shown (Fig. A1-R1a). The next time step (Fig. A1-R1b) confirms that upstream air needs to be colder for descent to the downstream bottom. The subsequent time steps (c-e) point to a problem with the choice of the upstream and downstream locations. I marked "cap" to show the top of downstream foehn layers. They are mostly well below the lowest possible crossing elevation and indicate that the upstream had been significantly modified by the many ups and downs between Milano and Vaduz as Fig. 3 of the manuscript shows. Milano-Vaduz is actually one of the longest distances where foehn descent is modeled..
   b. **Profile locations:** Therefore I suggest redoing the figures for a downstream location within the subregion d2, where the majority of trajectories descend much closer to the Alpine crest (Fig. 3 of manuscript) and use the computed trajectories to place the upstream location about 20 km upstream of the Alpine crest. Then add and discuss the figure in the main text of the manuscript.
2. **Hydraulic response and virtual topography:** The carefully prepared Figs. R3 and R4 (even with an inset of the cross-section location!) are a big help! Thanks! However, I disagree with their interpretation.
   a. **Descent limited to difference in potential temperature:** These figures actually show that the upstream air can only descend approximately as far as its level of neutral buoyancy on the downstream side! I marked up Fig. R3c-h and attach it as Fig. A2-R3. The obstacle I refer to In the following is between km 30 and 40 in the figure. In the first

cross section (left column, Fig. A2-R3c,e,g), the 292 K isentrope marked up in orange rises upstream as time progresses, i.e. the upstream air becomes colder. Between 5 UTC and 9 UTC the upstream air becomes still colder whereas the air downstream warms as is visible by the sinking of the 290 K and 288 K isentropes close to the next obstacle. In the final time step shown at 09 UTC, the 292 K isentrope has risen just far enough to cross the obstacle and can descend fairly far downstream with accompanying higher flow speeds. In the second cross section (second column, Figs. A2-R3d,f,h), a similar upstream cooling is shown by the rise of the 294 K isentrope (marked up in orange) and needed before the air can descend further downstream. The momentum of the descent is sufficiently large to *under*shoot the level of its neutral buoyancy and thus deform the isentrope downwards closest to the slope (which is reminiscent of positively buoyant air parcels in convection *over*shooting their level of neutral buoyancy).

b. **Waves are a response to virtual topography:** Fig. A2-R3 actually disentangles the seeming chicken-and-egg question of whether (gravity) waves modify the virtual topography or whether the waves are triggered by the virtual topography. A black outline in the second cross section of Fig. A2-R3 shows the region where the answer becomes obvious. There is no wave above the actual real topography. The wave is in response to the descending flow and the shape of the virtual topography that it causes. The wavelength corresponds to the virtual topography (an inverted peak) downstream of the real peak. For a further discussion, see Armi and Mayr (2011, section 4c) and Armi and Mayr (2015, section 3b first paragraph).

c. **Key features of hydraulic flow**: Focusing just on the last time step and the region between km 25 and 45 in Fig. A2-R3(g, h), one finds these key features of hydraulic flow: (i) descent of the overflowing layer already ahead of the hydraulic control location (= peak), (ii) asymmetric flow across the obstacle with accelerating flow on the downstream side, (iii) a rebound in a hydraulic jump to the conditions further downstream, and (iv) a less stably stratified and slow layer on the downstream side (between 298 K and 300 K) separating the foehn flow from the flow aloft.

Parts of Figs. R3 (or R4) should also be included in the final manuscript to discuss this topic.

References:

Armi, L. & Mayr, G.J. (2011): The Descending Stratified Flow and Internal Hydraulic Jump in the Lee of the Sierras. *Journal of Applied Meteorology and Climatology*, **50**, 1995–2011, https://doi.org/10.1175/JAMC-D-10-05005.1.

Armi, L. & Mayr, G. J. (2015): Virtual and Real Topography for Flows across Mountain Ranges. *Journal of Applied Meteorology and Climatology*, **54**, 723–731, https://doi.org/10.1175/JAMC-D-14-0231.1.

Mayr, G. J., & Armi, L. (2010). The influence of downstream diurnal heating on the descent of flow across the Sierras. *Journal of Applied Meteorology and Climatology*, *49*(9), 1906-1912. https://doi.org/10.1175/2010JAMC2516.1

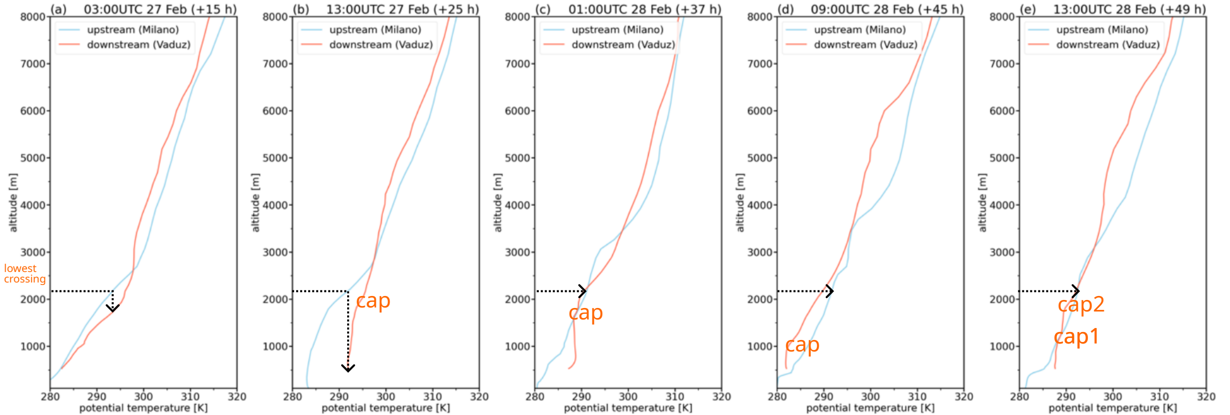
(a) 03:00UTC 27 Feb (+15 h)
(b) 13:00UTC 27 Feb (+25 h)
(c) 01:00UTC 28 Feb (+37 h)
(d) 09:00UTC 28 Feb (+45 h)
(e) 13:00UTC 28 Feb (+49 h)
upstream (Milano)
downstream (Vaduz)
altitude [m]
potential temperature [K]
lowest crossing
cap
cap
cap
cap2
cap1

Fig. A1-R1

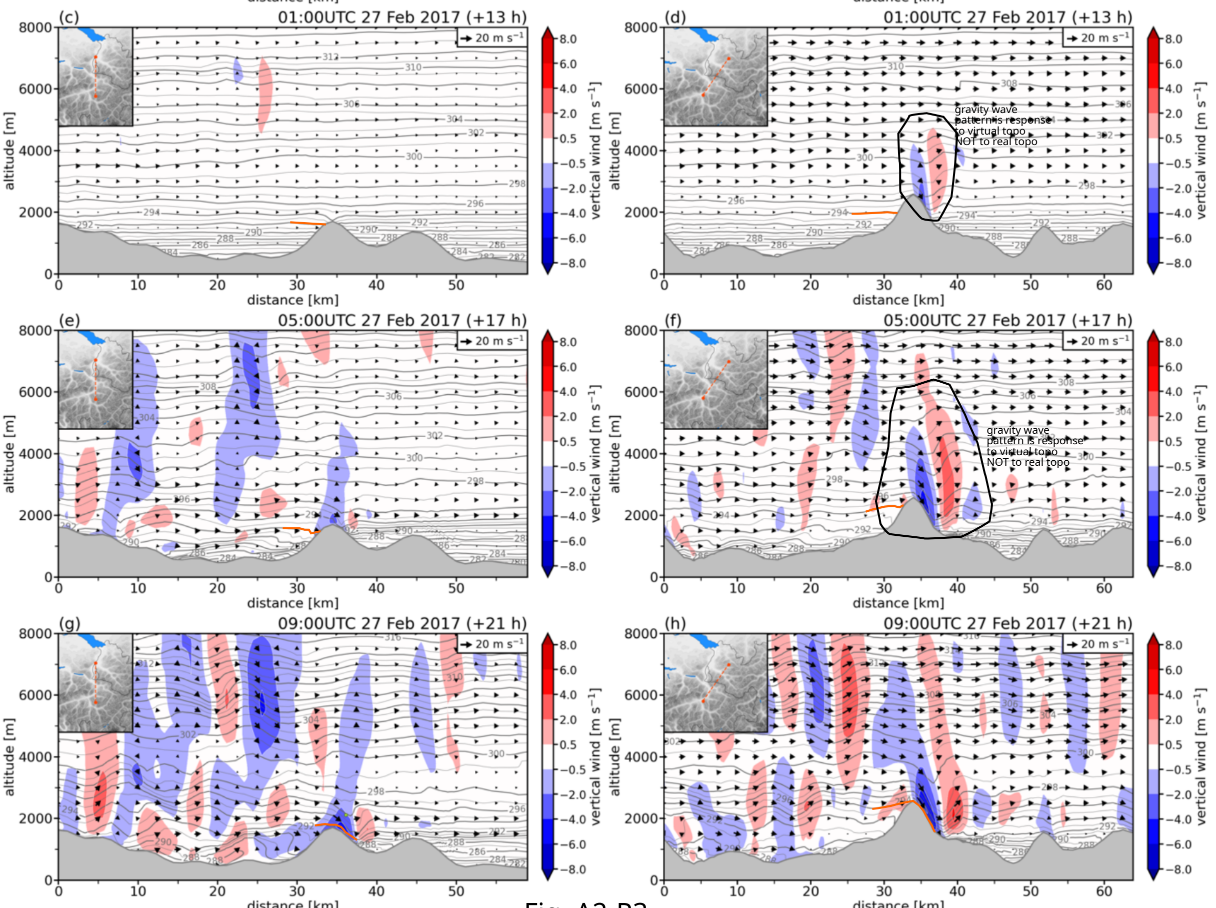

(c) 01:00UTC 27 Feb 2017 (+13 h)
(d) 01:00UTC 27 Feb 2017 (+13 h)
gravity wave pattern is response to virtual topo NOT to real topo
(e) 05:00UTC 27 Feb 2017 (+17 h)
(f) 05:00UTC 27 Feb 2017 (+17 h)
gravity wave pattern is response to virtual topo NOT to real topo
(g) 09:00UTC 27 Feb 2017 (+21 h)
(h) 09:00UTC 27 Feb 2017 (+21 h)
20 m s⁻¹
altitude [m]
distance [km]
vertical wind [m s⁻¹]

Fig. A2-R3